



UVA LEDs and solar light photocatalytic oxidation/ozonation as a tertiary treatment using supported TiO₂: With an eye on the photochemical properties of the secondary effluent

Manuel Figueredo ^a, Eva M. Rodríguez ^{a,*}, Eduardo M. Cordero ^b, Fernando J. Beltrán ^a

^a Departamento de Ingeniería Química y Química Física, Instituto Universitario de Investigación del Agua, Cambio Climático y Sostenibilidad (IACYS), Universidad de Extremadura, Avda. Elvas S/N, 06006 Badajoz, Spain

^b Departamento de Ingeniería Eléctrica, Electrónica y Automática, Escuela de Ingenierías Industriales, Universidad de Extremadura, 06006 Badajoz, Spain

ARTICLE INFO

Editor: Kaimin Shih

Keywords:

Supported TiO₂
Photocatalytic oxidation/ozonation
UVA LEDs and solar radiation
Pharmaceuticals
Secondary effluent
Indirect photolysis

ABSTRACT

Photocatalytic oxidation/ozonation of a mixture of eight pharmaceuticals added to a secondary effluent, SE, of an urban wastewater treatment plant has been studied using TiO₂ supported on commercial Al₂O₃/SiO₂ ceramic foams. As radiation source UVA LEDs (365 nm) or solar radiation was used. Pharmaceuticals were added at high (1 mg L⁻¹ each) or relatively low (50 µg L⁻¹ each) concentration, contributing 25% and 1.5% to the initial TOC, respectively. Under both types of radiation, the photolysis of SE generated reactive species capable of degrading the contaminants (indirect photolysis), this effect being greater at lower initial concentration of pollutants. Lower concentration of contaminants also favoured their degradation and the SE mineralization by photocatalytic oxidation, whereas its effect on ozonation was low. The best results were obtained by photocatalytic ozonation, especially in terms of COD removal, without observing any synergism or antagonism between O₃/Radiation and TiO₂/Radiation systems. In SE, the performance of the supported catalyst resulted much better than that of suspended TiO₂ P25, which showed almost no activity in this matrix. Through different cycles of reuse, the stability of the supported catalyst was confirmed.

1. Introduction

There is a huge amount of information published on photocatalytic removal of water contaminants of different nature, in most cases using suspended photocatalysts and being titania the most used [1–3]. Also, different studies about the simultaneous application of UV radiation, suspended photocatalysts and ozone (photocatalytic ozonation) reveal the existence of certain synergism between systems [4–8]. However, many of these photocatalytic oxidation/ozonation works have been carried out in ultrapure water, so their results cannot be extrapolated to actual wastewaters due to the strong effect of this matrix on the agglomeration/aggregation and activity of the catalyst particles [8–10]. Besides, catalyst separation from water by any mean (membranes, neutralization/coagulation, centrifugation, etc. [11,12] seriously compromises the viability of these processes. In spite of the studies that many research groups are conducting to prepare photocatalysts with magnetic properties [13,14], everything points to that, to be a reality, the implementation of photocatalytic processes will require the use of

immobilized materials, using different supports (glass, silica, polymers, alumina, hollow fiber membranes, etc) and techniques (dip-coating, photo-etching, electrophoretic deposition, etc.) [15–17]. The photocatalytic activity of different supported materials has been tested in ultrapure water using model compounds [18,19], resulting clearly lower than that of suspended catalysts [19]. However, if the goal of these processes is to remove micropollutants from secondary effluents, the effect of this matrix on supported catalysts (i.e. already aggregated and no scattering effect) is expected to be less important than on suspended ones, so the comparison results can totally differ [20,21]. Therefore, it is worth focusing efforts on studying the behavior of supported catalysts in real effluents. In addition, if the water is to be doped with pollutants for research purposes, the further their concentration from the real one is, the lesser transferable the results will be. The added contaminants and/or their degradation intermediates can absorb radiation (diminishing the fraction that incides on the catalyst), and/or be a large sink for ozone or other reactive species, preventing/reducing their participation in other reactions. Evenmore, at high concentration the added

* Corresponding author.

E-mail address: evarguez@unex.es (E.M. Rodríguez).

<https://doi.org/10.1016/j.jece.2022.107371>

Received 7 September 2021; Received in revised form 28 December 2021; Accepted 9 February 2022

Available online 11 February 2022

2213-3437/© 2022 The Author(s).

Published by Elsevier Ltd.

This is an open access article under the CC BY-NC-ND license

(<http://creativecommons.org/licenses/by-nc-nd/4.0/>).

compounds can hide the photochemistry of the secondary effluent and its role (positive or negative) in the elimination of micropollutants. In this sense, under sunlight, the organic matter present in sewage effluents (EfOM) generates excited triplet states ($^3\text{EfOM}^*$) of higher energy than those corresponding to natural organic matter (NOM), the quantum yield of EfOM photolysis in terms of generation of reactive oxygen species (ROS: $^1\text{O}_2$, O_2^* , H_2O_2 , HO^*) being also higher [22–26]. In addition to EfOM, under solar radiation some inorganic substances present in the effluent can contribute to the formation of ROS, as it is the case of nitrate that photolyzes at $\lambda < 340$ nm and generates HO^* [27].

Considering all the above, in this work TiO_2 photocatalysts supported on commercial $\text{Al}_2\text{O}_3/\text{SiO}_2$ foams have been prepared and used, alone or combined with ozone, to treat the secondary effluent of an urban wastewater treatment plant spiked with a mixture of pollutants at high (1 mg L^{-1} each) and relatively low ($50 \mu\text{g L}^{-1}$ each) concentration. UVA LEDs of high irradiance (emitting mainly at 365 nm) and solar radiation were used as radiation sources, and the contribution of EfOM to indirect photolysis of the compounds determined as a function of their concentration and the type of radiation.

2. Materials and methods

2.1. Reagents

All the reagents including the selected contaminants/probe compounds (acetaminophen, ACE; antipyrine, ANT; caffeine, CAF; diclofenac sodium salt, DIC; hydrochlorothiazide, HYD; ketorolac tromethamine, KET; metoprolol tartrate, MET; oxalic acid dihydrate, OXAL; primidone, PRM; and sulfamethoxazole, SUL) were of analytical grade (from Sigma-Aldrich, Fluka biochemika, Merck or Panreac Química) and used as received. TiO_2 P25 Aeroxide® was from Evonik Industries (Essen, Germany). Ultrapure water (UPw) was produced by a Millipore Milli-Q® academic system (Darmstadt, Germany). Pressurized oxygen (purity > 99.5) was supplied by Linde.

The SE was taken from the secondary sedimentation unit of Rincón de Caya municipal wastewater treatment plant (Badajoz, Spain), after an activated sludge biological oxidation. The effluent was then filtered (Whatman, grade 1) and frozen until use. Main characteristics of SE were: pH_0 8.2–8.4; $\text{COD} \sim 36 \text{ mg O}_2 \text{ L}^{-1}$; $\text{BOD}_5 \sim 11 \text{ mg O}_2 \text{ L}^{-1}$; TOC (filtered $0.45 \mu\text{m} = \text{DOC}$) $\sim 12 \text{ mg L}^{-1}$; inorganic carbon, $\text{IC} \sim 25 \text{ mg L}^{-1}$ (alkalinity $\sim 200 \text{ mg L}^{-1}$ as CaCO_3); turbidity $\sim 5 \text{ NTU}$; electrical conductivity $\sim 670 \mu\text{S cm}^{-1}$; $A_{254 \text{ nm}} = 0.24$ ($\text{SUVA} = 2.4 \text{ L (mg DOC m)}^{-1}$); $A_{365 \text{ nm}} = 0.05$; E_2/E_3 ($A_{254 \text{ nm}}/A_{365 \text{ nm}}$) = 4.7; $[\text{Cl}^-] \sim 90 \text{ mg L}^{-1}$; $[\text{SO}_4^{2-}] \sim 63 \text{ mg L}^{-1}$; $[\text{NO}_3^-] \sim 30 \text{ mg L}^{-1}$.

2.2. Photocatalyst synthesis

Ceramic foams (CF) of mullite ($\text{Al}_2\text{O}_3/\text{SiO}_2$ 20 ppi, Vukopor®, Lanik, Czech Republic), were used as support. From commercial pieces (nominal size $50 \times 50 \times 22 \text{ mm}$), 30 mm diameter $\times 22 \text{ mm}$ width and $3.1 \pm 0.3 \text{ g}$ average weight pieces were obtained. After several washings with boiling UPw and drying in a stove, TiO_2 immobilization was carried out by dip-coating (dip-coater ND-DC, Nadetech Innovations, Spain) following the procedure already reported [21]. Briefly, the pieces were submerged during 60 s in a 150 g L^{-1} TiO_2 P25 suspension in UPw at $\text{pH} 1.5$ (with HNO_3) at an immersion/emersion speed of 0.65 mm s^{-1} . Then, they were dried in an oven at $110 \text{ }^\circ\text{C}$ for 24 h and calcined at $500 \text{ }^\circ\text{C}$ for 2 h (heating rate: $5 \text{ }^\circ\text{C min}^{-1}$). Finally, the pieces were rinsed with UPw, dried and stored until use. In some cases, a new coating cycle (impregnation + calcination) was applied to observe its effect on the activity of the material. The synthesized materials have been called CF $_n$, where n (0, 1 or 2) indicates the number of TiO_2 coatings.

2.3. Experimental set-up and procedures

The experimental set-up consisted of a liquid recirculated (7.7 L h^{-1})

system between an ozonation tank and a tubular photoreactor. The ozonation tank (Pyrex®, 1.3 L capacity) was provided with inlets/outlets for gas and liquid and a sampling port. The photoreactor (borosilicate glass, 50 cm long $\times 2.8 \text{ cm}$ diameter, total volume 0.36 L), was located above the air-cooled radiation system equipped with a 6 LEDs string (LZ4-04UV00, LED ENGIN $\sim 3 \text{ W}$ radiant power each and λ_{max} 365 nm; $I_{\text{UVA},365 \text{ nm}} 3.73 \times 10^{-5} \text{ Einstein L}^{-1} \text{ s}^{-1}$ determined using nitrite $1.5 \times 10^{-4} \text{ M}$ as actinometer in presence of 0.25 M tert-butanol [28,29]). After introducing 23 CF $_n$ pieces (volume $\sim 0.04 \text{ L}$) the tube was covered with a stainless-steel reflector. For tests performed under natural solar radiation, the photoreactor was exposed to the sun by placing in the rear of the tube a CPC reflector tilted 37° (local latitude), thus offering an irradiated surface (S_{irrad}) of 0.05 m^2 . These tests were carried out during the central hours of sunny days with solar UVA irradiance values ($I_{\text{UVA}, \text{SOLAR}}$) of $30\text{--}45 \text{ W m}^{-2}$ measured with an ACADUS85 radiometer (Ecosystem-Environmental Services S.A., Barcelona, Spain). Fig. S1 (Supplementary material) shows some pictures of the installation.

Ozone was obtained from an Anseros Ozomat Com AD-002 generator fed with 15 L h^{-1} oxygen to get an ozone concentration of 10 mg L^{-1} in the exiting gas.

The procedure followed to carry out the different tests is described in Text S1. A given volume of a concentrated stock solution ($100\text{--}500 \text{ mg L}^{-1}$ in UPw) of each pure compound (that is, taking into account the salt content in case of DIC, KET and MET) was added to the water matrix (UPw or SE) to get the final desired concentration (1 or 0.05 mg L^{-1} each). According to their molecular structures and concentration (see Table 1), the TOC corresponding to the added compounds was $\sim 4 \text{ mg L}^{-1}$ and $\sim 0.2 \text{ mg L}^{-1}$ for mixtures of 1 and 0.05 mg L^{-1} each, contributing to 25% and 1.5% of initial TOC in SE, respectively.

To get an initial idea of the activity of CF $_n$ materials, some preliminary tests were carried out in UPw using primidone (14 mg L^{-1}) or dihydrated oxalic acid (35 mg L^{-1}) as probe compounds.

2.4. Analytical methods

The following techniques were applied for CF $_n$ material characterization: WDXRF for elemental composition and TiO_2 content (S8 Tiger 4 K WDXRF spectrometer, Bruker®); Nitrogen adsorption-desorption isotherms at -196°C for catalyst surface area (Autosorb iQ2-C, Quantachrome); and scanning electronic microscopy (SEM) for morphology and topography of the material surface (Quanta 3D FEG-FEI).

Before analysis, aqueous samples were filtered ($0.45 \mu\text{m}$ PVDF, Millipore) and possible remaining dissolved ozone purged by air. Concentration of the selected contaminants was determined by HPLC-DAD (Hitachi, Elite LaChrom, San Jose, CA, USA), in a C-18 Phenomenex ($3 \times 150 \text{ mm}$, $5 \mu\text{m}$) column. Analysis conditions, retention times and detection and quantification limits (LD and LQ, respectively) are shown in Table S1. For determination of organic and inorganic carbon content a TOC-VSCH (Shimadzu) analyzer was used. COD was measured using Hach Lange LCK414 cuvette test while for dissolved ozone concentration the indigo method was applied [41]. Finally, ozone (inlet and outlet) gas concentration was monitored by an Anseros Ozomat GM-6000 Pro analyser.

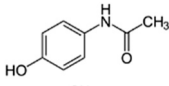
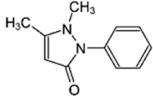
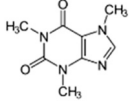
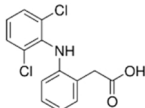
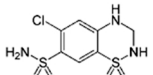
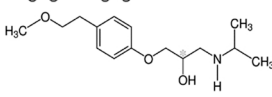
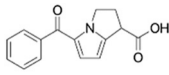
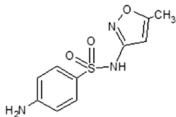
3. Results and discussion

3.1. Characterization of materials and preliminary tests on photocatalytic activity

3.1.1. Characterization of materials

The results obtained from WDXRF analysis are shown in Table 2. As observed, a small amount of TiO_2 (0.59% w/w) was present in the original foams (CF0) that increased to 4% and 10.7% in CF1 and CF2, respectively. Since the photoreactor was filled with 23 foam pieces, given the average weight of original foams, the total estimated amount of TiO_2 in the photoreactor was 0.41, 2.8 and 7.6 g using CF0, CF1 and

Table 1Selected compounds, molecular structures, pKa values and rate constant of their reactions with ozone (k_{O_3}) and hydroxyl radical ($k_{HO\cdot}$).

Compound (pure)	Molecular structure	pKa*	k_{O_3} (pH 8) $M^{-1}s^{-1}$	$k_{HO\cdot}$, $M^{-1}s^{-1}$
Acetaminophen $C_8H_9NO_2$ PM 151.16		9.4	3.8×10^7 [30]	$(2.2-7.1) \times 10^9$ [31]
Antipyrine $C_{12}H_{11}N_2O$ PM 188.23		1.4	5.3×10^4 [32]	$(4.9-7.9) \times 10^9$ [31,33]
Caffeine $C_8H_{10}N_4O_2$ PM 192.19		10.4	650 [34]	$(4.1-6.9) \times 10^9$ [31]
Diclofenac $C_{14}H_{11}NCl_2O_2$ PM 296.33		4.2	6.8×10^5 [32]	7.5×10^9 [35]
Hydrochlorothiazide $C_7H_8N_3ClO_4S_2$ PM 297.83		7.9	2.5×10^4 [36]	5.7×10^9 [36]
Metoprolol $C_{15}H_{25}NO_3$ PM 267.37		9.6	2.1×10^4 [32]	$(6.8-8.4) \times 10^9$ [31,37]
Ketorolac $C_{15}H_{13}NO_3$ PM 255.27		3.5	3.5×10^5 [38]	NA
Sulfamethoxazole $C_{10}H_{11}N_3O_3S$ PM 253.28		5.7	5.7×10^5 [39]	$(5.5-8.5) \times 10^9$ [31]

*From Rosal et al. [40]. NA: Not available.

Table 2

Composition of CFn (wt%) according to WDXRF analysis.

Compound	CF0	CF1	CF2	CF1 (used)
Al ₂ O ₃	69.0	65.0	62.1	65.9
SiO ₂	26.8	27.3	23.9	26.0
MgO	1.51	1.71	1.39	1.56
TiO ₂	0.59	3.99	10.7	4.48
K ₂ O	0.57	0.56	0.53	0.57
Na ₂ O	0.54	0.56	0.53	0.42
Fe ₂ O ₃	0.44	0.53	0.41	0.52
CaO	0.38	0.38	0.36	0.37

CF2, respectively.

Nitrogen adsorption isotherms revealed low specific surface: 0.226 m² g⁻¹ (CF0), 1.965 m² g⁻¹ (CF1) and 3.032 m² g⁻¹ (CF2). Although the amount of TiO₂ P25 increased with the coating cycles, a minimum development of surface was noticed given the aggregation of the catalyst.

Figs. S2–S4 show SEM images corresponding to CF0, CF1 and CF2. From these images it is deduced that TiO₂ deposition on foam surface was irregular, TiO₂ coating thicknesses ranging from 5 μm to 10 μm, indicating multilayer deposition. This means that a fraction of the supported catalyst will not be exposed to radiation.

3.1.2. Preliminary tests on photocatalytic activity

To get an initial idea about the photocatalytic activity of CFn, its behavior in UPw was compared with that of a TiO₂ P25 suspension using UVA LEDs as radiation source. Primidone ([PRM]₀ = 14 mg L⁻¹, [TOC]₀ ~ 9 mg L⁻¹, pH₀ ~ 6) and dihydrated oxalic acid ([OXAL]₀ 35 mg L⁻¹, [DOC]₀ ~ 7 mg L⁻¹, pH₀ ~ 3.5) were selected as test compounds. The former because its photocatalytic degradation using suspended TiO₂ P25

is caused by hydroxyl radicals diffused into the liquid bulk [8,42] and the latter because, at pH < pH_{pzc}, its photocatalytic removal goes through adsorption and positive hole oxidation at the catalyst surface [8, 43,44]. Neither PRM nor OXAL absorb 365 nm radiation.

Adsorption of PRM (30 min in the dark) on the different materials (CF0, CF1, CF2 or 10–100 mg L⁻¹ de P25) was negligible. The changes with time of PRM normalized concentration during the photocatalytic processes using CFn/UVA and P25/UVA are shown in Fig. S5. According to this figure, in UPw, CF1 activity in terms of HO[•] production in the bulk water was low and comparable to that of 10 mg L⁻¹ TiO₂ P25 suspension. The activity of CF0 was null and that of CF2 quite similar to CF1.

In the case of OXAL, after 30 min of contact in the dark, its adsorption on CF0 and 100 mg L⁻¹ TiO₂ P25 suspension was negligible (< 1%) and increased to 17% and 40% for CF1 and CF2, respectively. Given the high tendency of OXAL to adsorb on TiO₂ and form complexes [44], the differences between the amount of OXAL adsorbed onto CF1 and CF2 would be related to its adsorption isotherm [45]. The evolution of the normalized concentration of OXAL during CFn/UVA and P25/UVA tests is shown in Fig. S6, being very similar for CF1, CF2 and P25. Therefore, in UPw, the h⁺ production capacity of the prepared materials is comparable to that of a 100 mg L⁻¹ TiO₂ P25 suspension. From Fig. S6 a certain activity of CF0 is deduced. Although this could be related to the presence of a small amount of TiO₂ in the commercial foams (~ 0.6%, Table 2), in acidic conditions the formation and further photolysis of ferryxalate from interaction between OXAL and Fe₂O₃ present in the commercial foams (Table 2) cannot be disregarded. In CF1 and CF2 this interaction would be much lower as it is prevented by the TiO₂ coating.

According to these previous results, in UPw: i) TiO₂ aggregation state in the prepared materials makes it difficult for the HO[•] generated on the surface to diffuse into the solution, being CF1 and CF2 photocatalytic

activity in terms of HO[•] generation in the bulk similar to that of 10 mg L⁻¹ TiO₂ P25 suspension; ii) as far as h⁺ generation is concerned, CF1 and CF2 photocatalytic activity was comparable to that of 100 mg L⁻¹ TiO₂ P25 suspension; iii) Although TiO₂ content in CF2 was higher than in CF1, its photocatalytic behavior was practically the same. Bearing this in mind, CF1 was chosen to continue the study.

3.2. Photolysis of the selected contaminants. Influence of type of radiation and water matrix

Main aspects that affect the photodegradation of a given compound in water are: i) the overlapping of its absorption spectrum with the emission spectrum of the radiation source; ii) the intensity of radiation absorption (molar absorptivity) and quantum yield; iii) the intensity of radiation; and iv) the presence or formation in the water matrix of photosensitizers (indirect photolysis).

Fig. S7 shows molar absorptivity (ϵ_λ) of the selected contaminants in the 300–400 nm range, in UPw at pH ~ 6 and in an aqueous solution of 2 mM NaHCO₃ at pH 8.5 (pH and alkalinity similar to that of SE). According to this figure, an influence of pH on ϵ_λ was only observed in the case of SUL, with lower ϵ_λ values at pH 8.5. The absorption spectrum of the SE is shown in Fig. S8, and the terrestrial solar and UVA LEDs emission spectra in Fig. S9. In view of Figs. S7 and S9, under UVA (365 nm) direct photolysis of KET would be possible, and that of KET, HYD, DIC and SUL under solar radiation. Considering Figs. S8 and S9, SE photolysis can take place under both types of radiation.

The photolytic degradation of the selected pollutants (mixtures of 1 mg L⁻¹ of each pure compound) was determined as a function of the water matrix (UPw or SE) and type of radiation (UVA₃₆₅ LEDs or solar radiation, named UVA and SOLAR, respectively, thereafter). Fig. S10 shows the evolution of the global normalized concentration of contaminants during these tests. Experimental results were fitted to pseudo first order kinetics. In Table S2 the values of pseudo first order rate constants, k_{Obs} , obtained at the different conditions are compiled. These values are compared in Fig. 1. In tests performed using SOLAR, the evolution over time of $I_{UVA, SOLAR}$ and the reaction temperature were practically the same (see Fig. S11).

Under UVA, according to Fig. 1, in UPw, degradation of KET (90% after 4 h) and DIC (45% after 4 h) was observed. However, if molar absorptivity of DIC at 365 nm (Fig. S7) and quantum yield are considered [46], its photolysis should be negligible. This was experimentally verified in UPw by exposing a 1 mg L⁻¹ DIC solution to UVA radiation, being 8% DIC removed after 4 h (not shown). Hence, in UPw, it is deduced that KET photolysis generates some reactive

intermediate/species capable to interact with DIC (indirect photolysis). According to Leo et al. [47] this intermediate could be ³KET* since KET contains a similar conjugation system to that of benzophenone. When the compounds were spiked in SE, all were degraded to a greater or lesser extent, especially ACE and DIC. For KET, k_{Obs} value was slightly lower than in UPw, which could be attributable to the absorption of UVA by SE. In any case, no doubt UVA photolysis of SE leads to the formation of reactive species capable to interact with the compounds, especially DIC, ACE and HYD, with degradations in the 65–85% range after 4 h.

Under SOLAR, all compounds but ANT and CAF were degraded to a greater or lesser extent in both matrices, with complete HYD and DIC removal after 4 h. In general, a slightly negative effect of SE matrix was observed. Hence, the absorption of solar radiation by the SE reduced the direct photodegradation of the pollutants, the reactive species generated from SE solar photolysis being unable to counteract this effect.

Compared to SOLAR, the higher degradation of ACE caused by SE photolysis under UVA could suggest a relationship between the nature of the reactive species generated from SE photolysis and the radiation wavelength. Nevertheless, these species seem to be less reactive towards ANT and CAF.

3.3. Supported photocatalyst and UVA LEDs or solar radiation for SE treatment by different processes

The SE containing the mixture of contaminants (1 mg L⁻¹ each) was treated by Radiation, CF1/Radiation, O₃, CF1/O₃, O₃/Radiation and CF1/O₃/Radiation systems, using UVA or SOLAR. For CF1/O₃, the results were similar to those of O₃ (not shown). After 30 min of contact with the catalyst in the dark, adsorption of pollutants and TOC was negligible.

3.3.1. Removal of contaminants

Fig. 2 (a, b) shows the changes with time of global normalized concentration of contaminants using UVA (Fig. 2a) and SOLAR (Fig. 2b).

As expected, CF1/Radiation was less effective than processes involving ozone. However, the clear differences observed between Radiation and CF1/Radiation systems indicate that the material presents photocatalytic activity. In Fig. 3a, for each contaminant, the values of k_{Obs} for these two processes are shown ($R^2 > 0.97$ in all cases). As it is deduced, the contribution of photolysis (direct and/or indirect) to the efficiency of the CF1/Radiation system to degrade the compounds was higher than 25% for ACE, KET and DIC using UVA; and for DIC and HYD using SOLAR.

Regarding ozone-based systems, no significant differences were

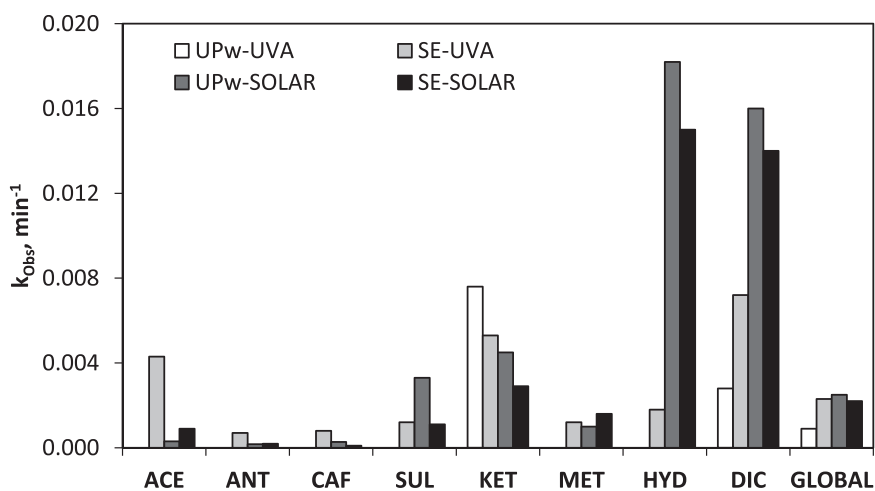


Fig. 1. Influence of the type of matrix (UPw or SE) and radiation (UVA or SOLAR) in the photolytic degradation of the selected contaminants. Experimental conditions: $[C_i]_0$ 1 mg L⁻¹ each; Q_{O_2} 15 L h⁻¹; Q_L 7.7 L h⁻¹; In UPw: $[TOC]_0 \sim 4$ mg L⁻¹; pH ~ 6; In SE: $[TOC]_0 \sim 16$ mg L⁻¹; pH 8.2–8.4; UVA: $I_{0,365\text{ nm}} = 3.73 \times 10^{-5}$ Einstein (L s)⁻¹ and $T = 20 \pm 2$ °C; SOLAR: $I_{UVA, SOLAR} = 30\text{--}45$ W m⁻², S_{irrad} 0.05 m² and T from ~ 20 °C to ~ 38 °C after 4 h.

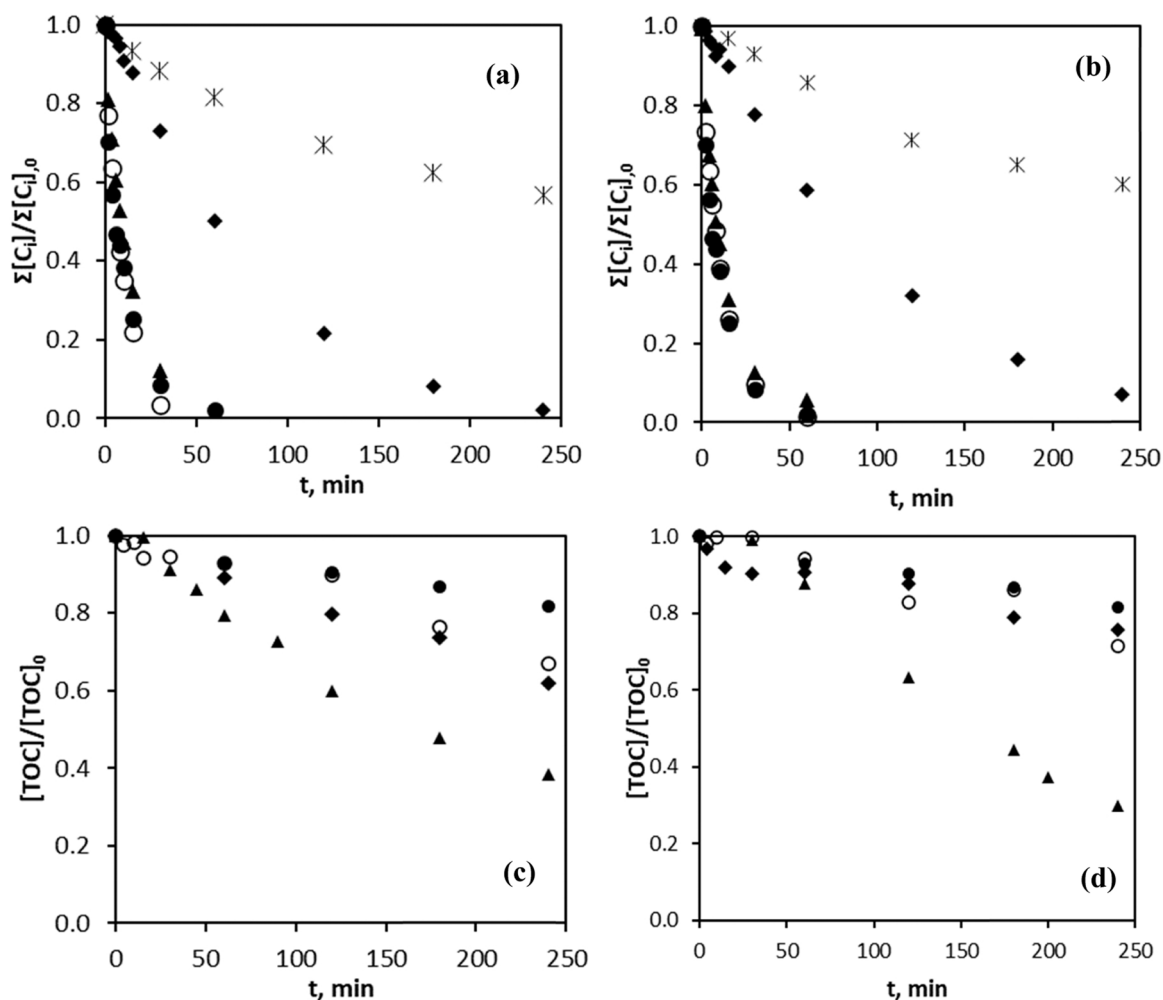


Fig. 2. Time evolution of normalized total concentration of contaminants (a, b) and TOC (c, d) during the application of different processes in SE using UVA (a, c) or SOLAR (b, d). Symbols: * Radiation; • O₃; ○ O₃/Radiation; ◆ CF1/Radiation; ▲ CF1/O₃/Radiation. Experimental conditions: $[C_i]_0$ 1 mg L⁻¹ each; $[TOC]_0 \sim 16$ mg L⁻¹; pH 8.2–8.4; Q_{O_2} or $Q_{O_2-O_3}$ 15 L h⁻¹; Q_L 7.7 L h⁻¹; $[O_3]_{in}$ 10 mg L⁻¹; UVA: $I_{0,365\text{ nm}} = 3.73 \times 10^{-5}$ Einstein (L s)⁻¹ and $T = 20 \pm 2$ °C; SOLAR: $I_{UVA, SOLAR} = 30\text{--}45$ W m⁻², $S_{irrad} = 0.05$ m² and T from ~ 20 °C to ~ 38 °C after 4 h. Note: simple ozonation was performed only at room T.

observed between them likely due to the moderate-high reactivity of the target compounds with ozone at the pH of SE. According to data shown in Table 1, this reactivity is moderate for CAF (k_{O_3-CAF} 650 M⁻¹ s⁻¹) and high for the rest of compounds (k_{O_3-C} values in the range 2.1×10^4 M⁻¹ s⁻¹ to 3.8×10^7 M⁻¹ s⁻¹). By simple ozonation, the disappearance rate of the pollutants followed an order similar to that of their reactivities with ozone (Fig S12). Even so, the combination of ozone with CF1/radiation (CF1/O₃/Radiation) had a slight positive effect as deduced from Fig. 3b, which shows k_{Obs} ($R^2 > 0.97$ in all cases) for each compound by O₃ and CF1/O₃/Radiation processes, together with the values of $k_{O_3-C_i}$ at pH 8. For all ozone-based systems, regardless of the presence of radiation, during the first 60 min (time needed for almost complete disappearance of all the contaminants, see Fig. 2 (a, b)), dissolved ozone concentration in the water fed to the photoreactor was very low ($\leq 3 \times 10^{-6}$ M, not shown). Therefore, the contribution of O₃-radiation and O₃-CF1/Radiation interactions to the degradation of the compounds can be ruled out.

3.3.2. Mineralization

Fig. 2 (c, d) show the variation with time of normalized remaining TOC during the application of different systems, using UVA (Fig. 2c) or SOLAR (Fig. 2d). UVA and SOLAR photolysis did not lead to any mineralization (not shown). As observed, the efficiency of O₃, O₃/Radiation and CF1/Radiation to remove TOC was relatively low, with mineralization percentages lower than 40% (using UVA) or 30% (using

SOLAR) in 4 h. At this time, TOC reduction by CF1/O₃/Radiation was 60% (UVA) and 70% (SOLAR), results in Fig. 2 (c, d) suggesting the existence of some sort of synergism between O₃/Radiation and CF1/Radiation only when solar radiation was applied. Again, given the very low ozone concentration in the water fed to the photoreactor during the application of CF1/O₃/Radiation system (see Fig. S13), this slight synergy would not be attributable to direct interactions between ozone-Radiation nor ozone-CF1/Radiation.

From Fig. 2 it can be concluded that for both global removal of compounds and mineralization, the efficiency of each system using a 6 LEDs UVA_{365 nm} string (~ 3 W radiant power each, total effective radiant power calculated as 12.2 W from actinometry) or solar radiation ($I_{UVA, SOLAR}$ 30–45 W m⁻² and S_{irrad} 0.05 m², that is, 1.5–2.25 W without considering the transmittance of glass or reflectance of aluminum), was quite similar.

3.4. Supported photocatalyst and UVA LEDs for SE treatment by different processes: Approach to real conditions

According to what has been discussed in previous sections, when working with mixtures of 1 mg L⁻¹ each contaminant in SE under UVA it is deduced that: i) KET and water matrix absorb radiation, which likely limits the photon flow reaching the catalyst surface; ii) the contribution of ROS generated from SE photolysis to the indirect photodegradation of

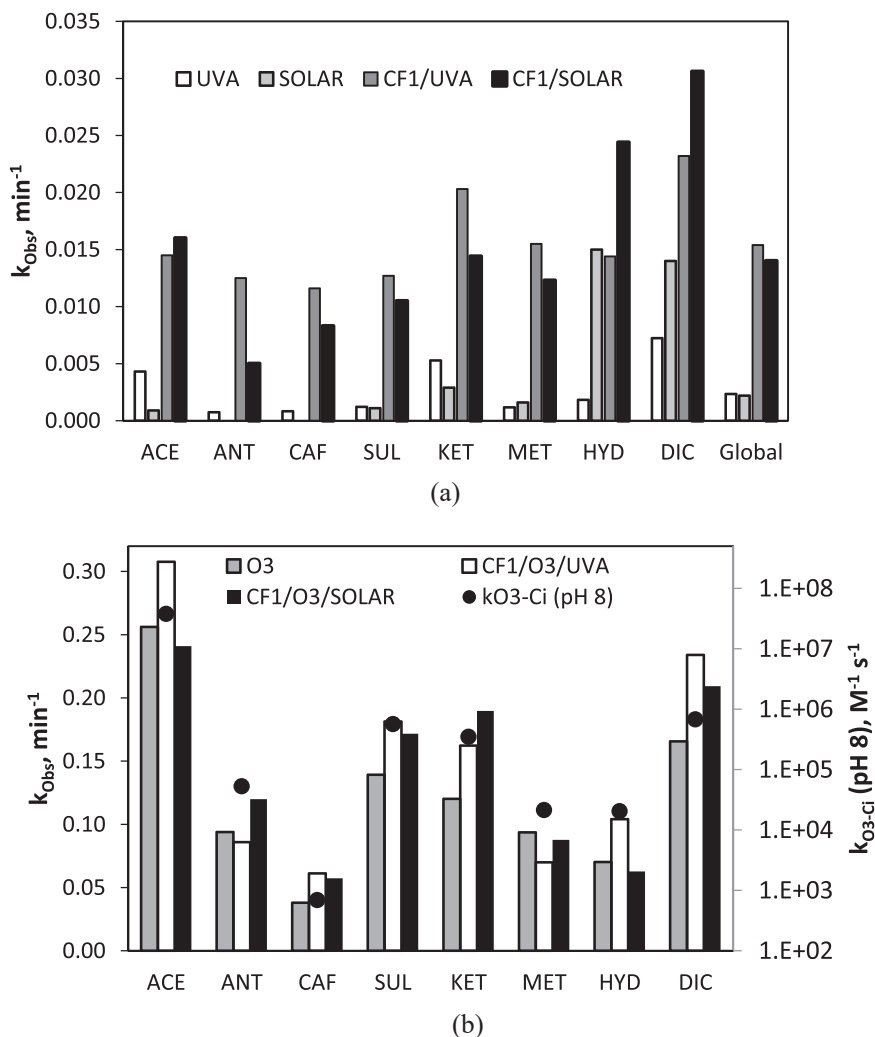


Fig. 3. Comparison of k_{obs} values for the selected contaminants in SE corresponding to (a) UVA, SOLAR, CF1/UVA and CF1/SOLAR systems; and (b) O₃, CF1/O₃/UVA and CF1/O₃/SOLAR systems, together with k_{O3-Ci} values calculated at pH 8. Same conditions as in Fig. 2.

the compounds could be affected by the concentration of the contaminants; and iii) the higher the concentration of the pollutants the higher the ozone demand (associated to parent compounds and their intermediates). At real conditions, the concentration of pollutants is much lower, in the ng L⁻¹ to µg L⁻¹ range [40,48–50], affecting all the aspects indicated above. Thus, a new experimental series was carried out applying the UVA, O₃, CF1/UVA and CF1/O₃/UVA systems to treat a mixture of 50 µg L⁻¹ of each pollutant in SE. These concentrations are, however, still higher than the real ones, but are within the lowest level the analytical equipments used in this work (HPLC-DAD) can detect and quantify, except for MET (see LD and LQ values in Table S1). For this reason, although MET was also added to the mixture, data related to its evolution during the treatments are not included.

Fig. 4a shows the variation with time of global normalized remaining concentration of contaminants corresponding to this experimental series. Discussion of the results are based on their comparison with those shown in Fig. 2a, obtained at similar conditions but adding 1 mg L⁻¹ of each compound to SE.

Firstly, the photolytic removal of contaminants can be highlighted (notice that only KET and SE matrix absorb at 365 nm, Figs. S7 and S8). Thus, a global reduction of 40% and 70% was reached after 1 and 4 h, respectively, much higher than 20% and 40% observed with 1 mg L⁻¹ each.

For each compound, Fig. 5a shows the effect of diminishing its initial concentration in the efficiency of the UVA process measured as k_{obs} (R^2

> 0.97 in all cases), where the ratio between k_{obs} (for 0.05 mg L⁻¹) and k_{obs} (for 1 mg L⁻¹) is also given. According to this figure, for CAF, ANT and KET ratios between 1 and 2 were obtained, which means a slight positive effect of lowering the initial concentration and absence of negative effect. For the rest of contaminants, the k_{obs} ratio was higher than 2, SUL, ACE and HYD presenting the highest (~ 4). Therefore, at the range of concentrations studied, the lower the initial concentration of pollutants the higher the steady-state concentration of ROS generated from the photolysis of SE.

According to Figs. 4a and 2a, for CF1/UVA, lowering the initial concentration of contaminants led to a significant decrease in the time needed to achieve the same overall removal percentage. In contrast, for ozone system, no practical effect was observed. For instance, when treating mixtures of 1 mg L⁻¹ each in SE, the time needed to reach 80% overall reduction of contaminants was 120 min (CF1/UVA) and 15 min (O₃) (Fig. 2a), whereas 30 min (CF1/UVA) and 15 min (O₃) were needed for mixtures of 50 µg L⁻¹ each (Fig. 4a). According to these results, at low initial concentration of the compounds the competition of the SE matrix for ozone is higher, but not for other ROS. In Fig. 5b, for each compound, k_{obs} values ($R^2 > 0.97$ in all cases) corresponding to CF1/UVA system are compared as a function of their initial concentration, together with the k_{obs} (0.05 mg L⁻¹)/ k_{obs} (1 mg L⁻¹) ratio. As observed, a 20-fold reduction in the initial concentration of contaminants resulted in a 4-fold increase in k_{obs} . The beneficial effect of combining ozone and CF1/UVA systems (i.e., CF1/O₃/UVA) was also greater at the lower

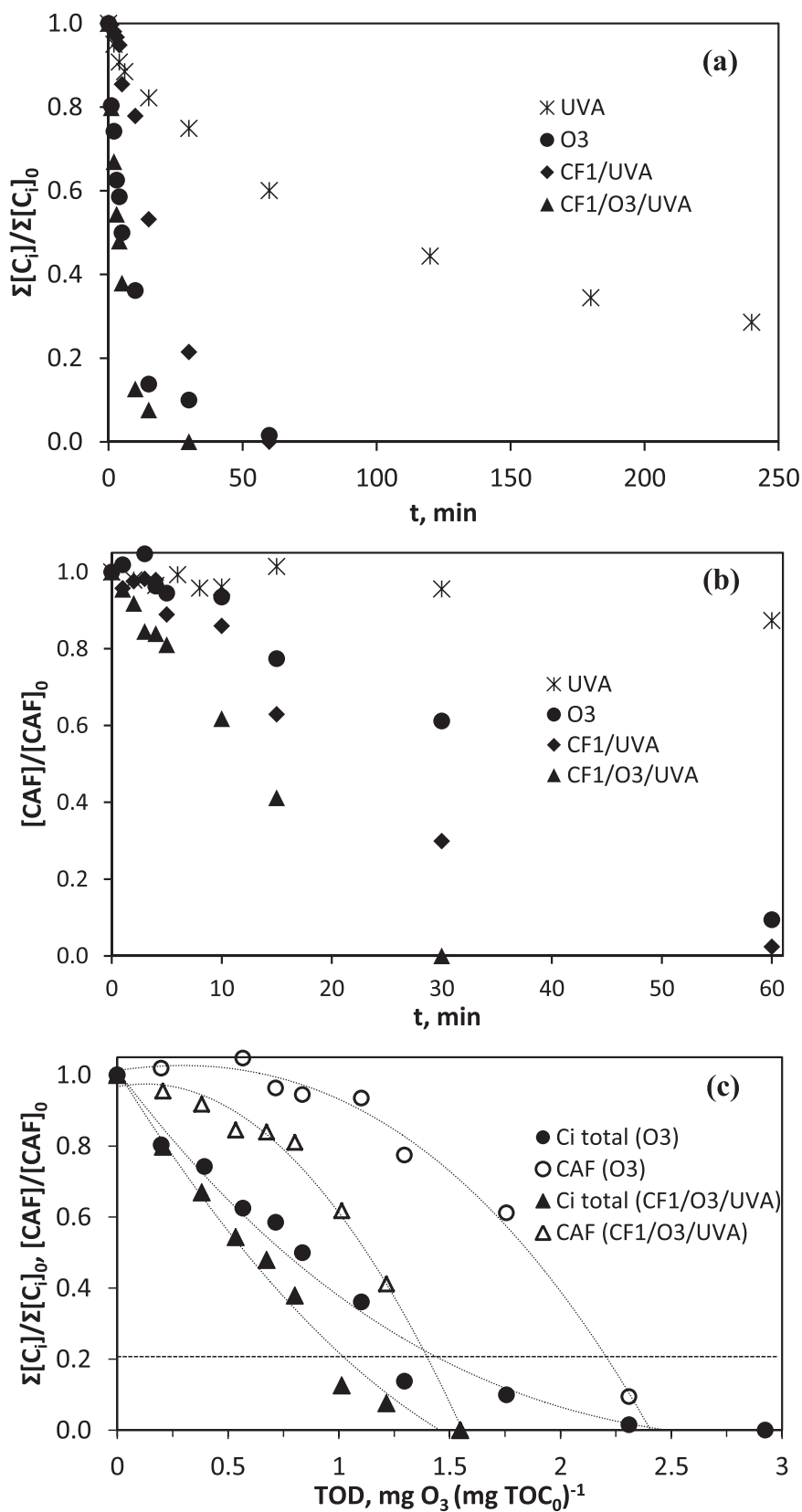


Fig. 4. Evolution of normalized total concentration of contaminants and CAF with time (a, b) and with TOD (c) during the application of different processes in SE. Experimental conditions: $[C_i]_0$ 0.05 mg L^{-1} each; $[\text{TOC}]_0 \sim 12.2 \text{ mg L}^{-1}$; pH 8.2–8.4; Q_L 7.7 L h^{-1} ; Q_{O_2} or $Q_{O_2-O_3}$ 15 L h^{-1} ; $[\text{O}_3]_{\text{in}}$ 10 mg L^{-1} ; $I_{0,365 \text{ nm}} = 3.73 \times 10^{-5} \text{ Einstein (L s)}^{-1}$; $T = 20 \pm 2 \text{ }^\circ\text{C}$. Lines in (c) are shown to guide the eye.

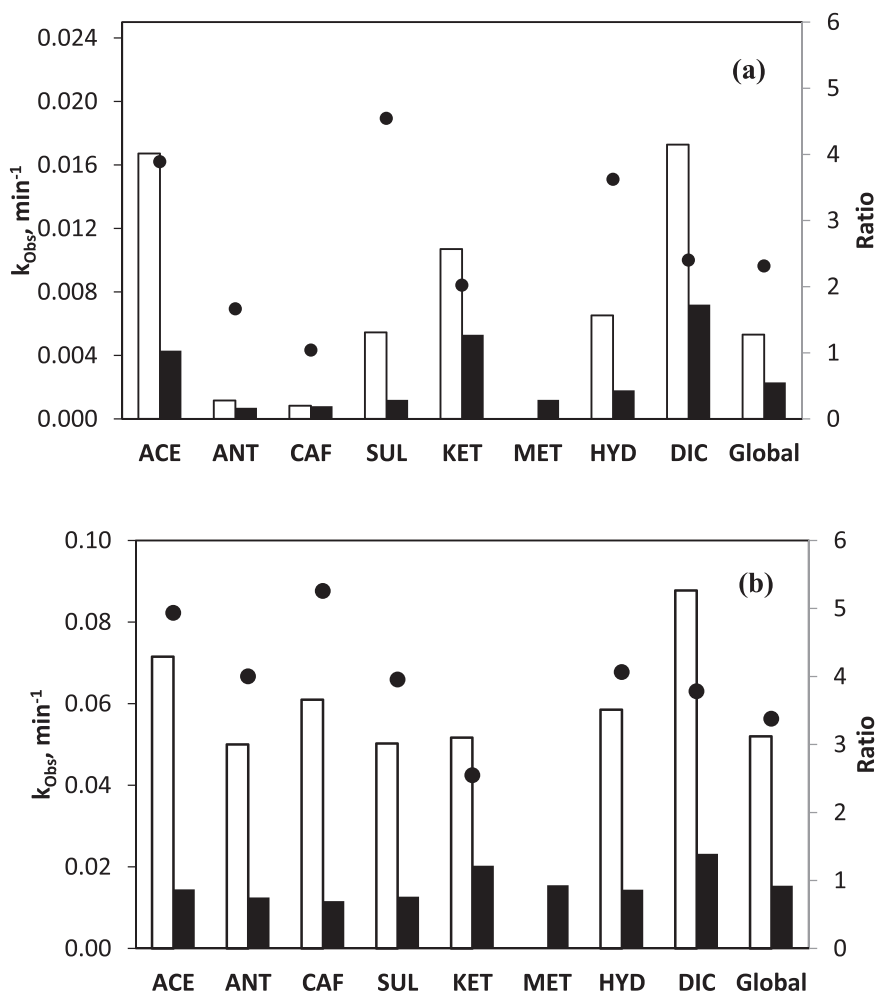


Fig. 5. Comparison of k_{obs} values for the selected contaminants in SE for mixtures of 0.05 mg L^{-1} each (empty bars) and 1 mg L^{-1} each (solid bars) during UVA (a) and CF1/UVA (b) processes. Symbols: \bullet $k_{\text{obs}}(0.05 \text{ mg L}^{-1})/k_{\text{obs}}(1 \text{ mg L}^{-1})$ ratio. Experimental conditions: $[\text{TOC}]_0 \sim 16 \text{ mg L}^{-1}$ (mixtures 1 mg L^{-1} each) and 12.2 mg L^{-1} (mixtures 0.05 mg L^{-1} each); pH 8.2–8.4; Q_{O_2} 15 L h^{-1} ; Q_{L} 7.7 L h^{-1} ; $I_{0,365 \text{ nm}} = 3.73 \times 10^{-5} \text{ Einstein (L s)}^{-1}$; $T = 20 \pm 2 \text{ }^\circ\text{C}$.

concentration studied, especially for the most resistant compounds to ozone attack. Fig. 4b confirms this conclusion when CAF, with the lowest $k_{\text{O}_3\text{-C}}$ value among the selected compounds (Table 1), is considered. As seen in Fig. 4b, the CF1/UVA system was even more effective than simple ozonation in degrading CAF, although the CF1/O₃/UVA combination was the one that led to the best results. Hence, compared to simple ozonation, to reach a given percentage of contaminant removal by CF1/O₃/UVA the amount of ozone that needs to be transferred to the water will be lower. This is clearly deduced from Fig. 4c that shows the variation with time of the global normalized concentration of pollutants and CAF as a function of the transferred ozone dose, TOD, expressed as $\text{mg O}_3 (\text{mg TOC}_0)^{-1}$, for O₃ and CF1/O₃/UVA systems. Compared to simple ozonation, the TOD needed to reach 80% global contaminant or CAF concentration removal by CF1/O₃/UVA was 33% lower.

According to these results, working with high concentration of contaminants (1 mg L^{-1} each) could mask the true activity of the photocatalyst because, among other reasons, the pollutants act as a large sink for the species generated during the photoexcitation, preventing their participation in other reactions. In this sense, lowering initial concentration of compounds exerted a positive effect on % TOC removal as deduced from Figs. 6a and 2c, where the changes of normalized TOC with time are shown. As observed, after 4 h, working at high and low initial concentration of pollutants, the % of TOC eliminated was 20% and 28% (O₃), 38% and 57% (CF1/UVA), and 62% and 76% (CF1/O₃/UVA), respectively. However, if the initial TOC content is considered ($\sim 16 \text{ mg L}^{-1}$ and 12.2 mg L^{-1} for mixtures of 1 and 0.05 mg L^{-1} of each

compound in SE), for each system, the amount of TOC removed (mg L^{-1}) resulted similar. This means that ozone and ROS consumption increased with the increase on pollutants concentration barely affecting the performance of each system. Only a slight influence on CF1/UVA performance was observed, the amount of TOC mineralized after 4 h being 6.1 mg L^{-1} and 7 mg L^{-1} , at high and low initial concentration of contaminants, respectively.

Contrary to mineralization, the efficiency of simple ozonation to reduce COD was high as shown in Fig. 6b. This is a logical result of the ability of ozone to transform the organics present in highly oxygenated ones (e.g. carboxylic acids, aldehydes, alcohols and ketones). Thus, by O₃, after 4 h, TOC and COD were reduced 30% and 50%, respectively. For CF1/UVA and CF1/O₃/UVA, differences between final TOC and COD reductions were not significant which means that, compared to ozonation, organic matter oxidation by these systems was simultaneous to mineralization. In the case of the CF1/O₃/UVA, a significant COD reduction in the first 60 min (42%) can be highlighted, which practically coincides with the sum of the reduction in COD obtained at that time through the individual processes (O₃, 24%; CF1/UVA, 17%).

Once more, for a given TOD, the CF1/O₃/UVA system was more efficient than O₃ alone to reduce TOC and COD. For example, according to Fig. 6c, for $3 \text{ mg O}_3 (\text{mg TOC}_0)^{-1}$ of TOD, ozonation led to $\sim 10\%$ TOC and 30% COD reduction, that increased to $\sim 50\%$ and 60%, respectively, by CF1/O₃/UVA.

When the SE doped with the lowest initial concentration of contaminants was treated by CF1/O₃/UVA, a measurable dissolved ozone

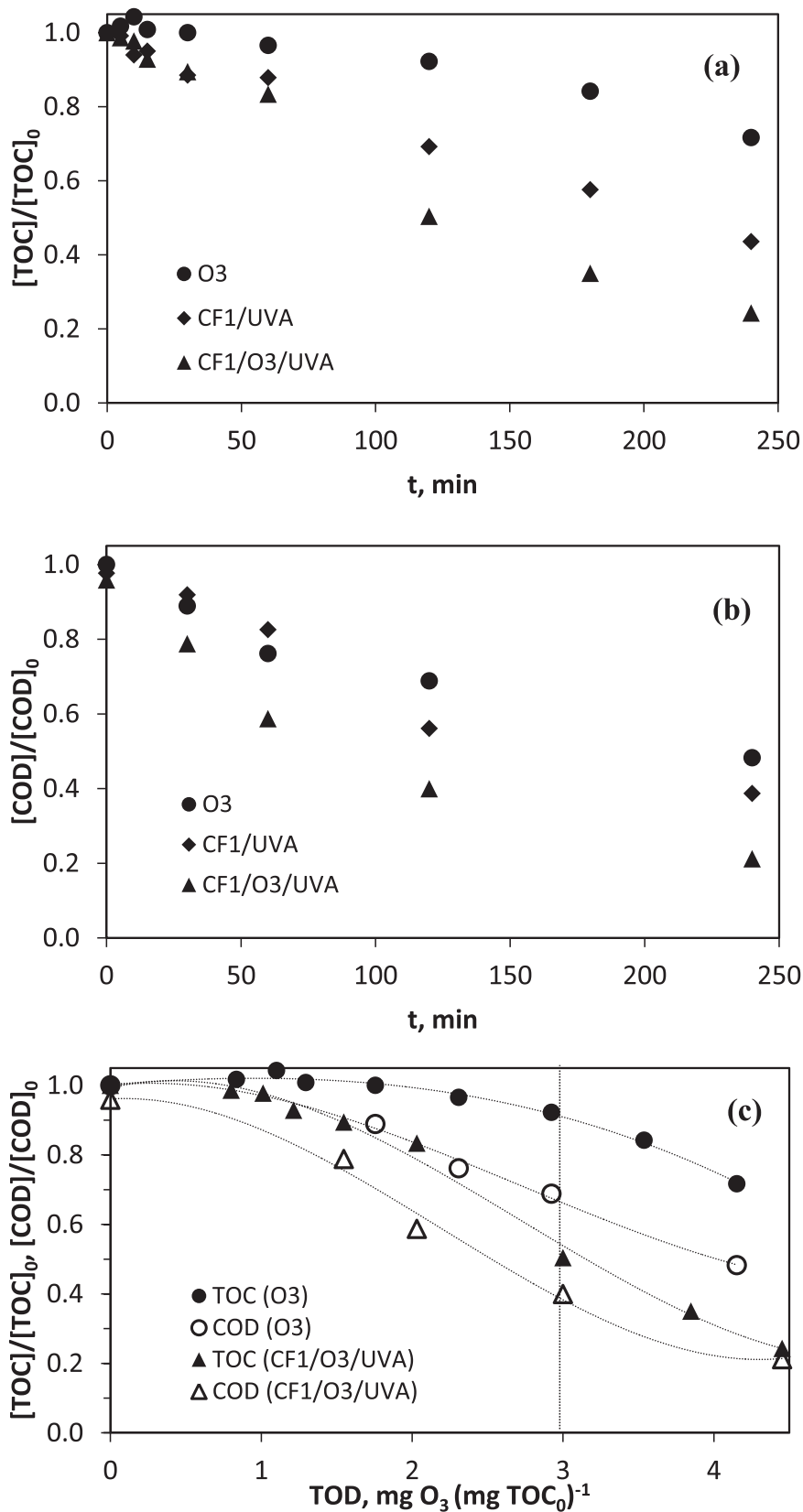


Fig. 6. Evolution of normalized TOC content and COD with time (a, b) and with TOD (c), during the application of different processes in SE. Same conditions as in Fig. 4. Lines in (c) are shown to guide the eye.

concentration was observed in the ozonation tank. This was undoubtedly due to the lower ozone demand corresponding to the contaminants added and their intermediates (see Fig. S15). However, a higher ozone concentration fed to the photoreactor did not lead to increased mineralization (expressed as mg L^{-1} TOC mineralized for a given TOD), suggesting a negligible contribution of O_3 -UVA or O_3 -CF1/UVA interactions to remove TOC. In summary, the results of this work show neither synergism nor antagonism between the O_3 and CF1/UVA systems.

3.5. Supported photocatalyst vs TiO_2 P25 suspension

Following the results shown and discussed in the preceding section, the use of CF1/UVA system could be a good option to remove micropollutants in SE, especially considering the easy separation of the catalyst from water. According to the preliminary tests (see Section 3.1.2), in UPw and using UVA, compared to 100 mg L^{-1} of suspended TiO_2 P25 the amount of HO^\bullet diffused into the bulk when CF1 was irradiated was much lower (see Fig. S5). However, this comparison must be established in the target matrix, that is, in SE. Therefore, SE containing 0.05 mg L^{-1} of each contaminant was treated by P25/UVA using 100 mg L^{-1} of TiO_2

P25. The results corresponding to UVA, CF1/UVA and P25/UVA systems are shown in Fig. 7. As observed, contrary to UPw, in SE the photocatalytic activity of CF1 was much higher than that of P25. Even more, when using P25/UVA the removal rate of contaminants (both global, Fig. 7a, or individual, Fig. 7b) practically coincided with those by UVA, and only in the case of ACE and DIC a slight positive effect of P25 was observed. In line with these results, while the efficiency of the powdered catalyst in terms of SE mineralization was null, 60% TOC was removed after 4 h using CF1.

3.6. Reuse of supported photocatalyst

To be implemented, an important feature of supported catalysts is their stability, thus allowing their reuse. To check this, the test performed treating the mixture of 1 mg L^{-1} each in SE by CF1/ O_3 /UVA was repeated three consecutive times, each run lasting 5 h. Fig. S16 shows the results obtained in terms of TOC changes with reaction time. According to these results, and in agreement with a previous work [21], the loss of efficiency was not significant which confirms a good catalyst stability. On the other hand, according to WDXRF analysis of reused CF1

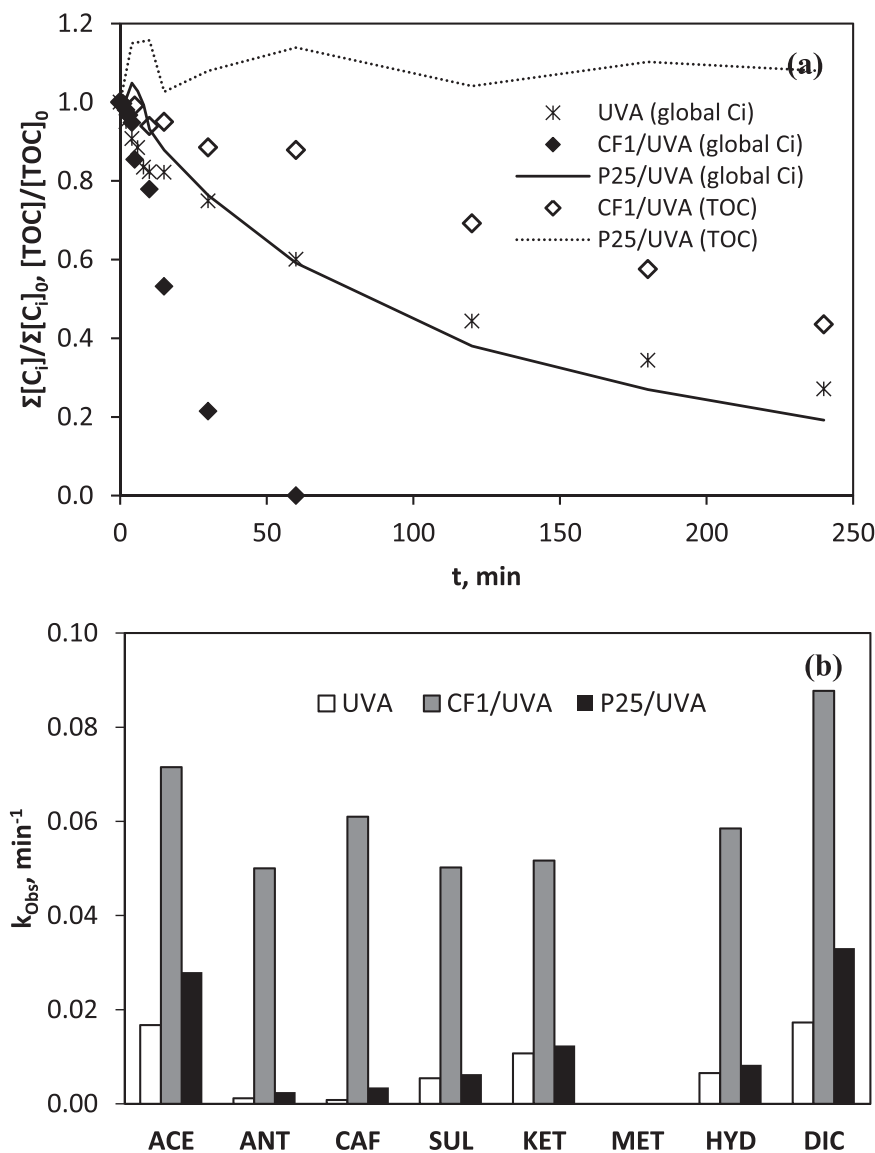


Fig. 7. Comparison of the efficiency of UVA, CF1/UVA and P25/UVA systems in terms of (a) global degradation of contaminants and TOC mineralization; (b) degradation of the selected compounds. Experimental conditions: $[C_i]_0$ 0.05 mg L^{-1} each in SE; $[\text{TOC}]_0 \sim 12.2 \text{ mg L}^{-1}$; pH 8.2–8.4; Q_{O_2} 15 L h^{-1} ; Q_L 7.7 L h^{-1} ; TiO_2 P25 100 mg L^{-1} ; $I_{0,365 \text{ nm}} = 3.73 \times 10^{-5} \text{ Einstein (L s)}^{-1}$; $T = 20 \pm 2 \text{ }^\circ\text{C}$.

(see Table 2), TiO₂ content resulted even higher than that of CF1 freshly prepared, which would be related to the heterogeneity of the coating.

4. Conclusions

Main conclusions of this work are:

- In UPw, the activity of supported catalysts in terms of generation of HO[•] in the liquid bulk was low and similar to that of 10 mg L⁻¹ TiO₂ P25 suspension. In terms of h⁺ generation, their activity was comparable to that of a 100 mg L⁻¹ TiO₂ P25 suspension. More than one coating did not increase the activity of the catalyst.
- Under UVA, photolysis of SE led to the formation of reactive species capable to interact with the compounds, especially DIC, ACE and HYD. Under SOLAR, the SE matrix reduced the extent of direct photolysis of the pollutants. This effect was not counteracted by the reactive species generated from SE photolysis.
- Working with a mixture of 1 mg L⁻¹ of each contaminant in SE, in terms of global removal of compounds and SE mineralization, for each radiation-based system its efficiency using 6 UVA LEDs (~3 W radiant power each) or solar radiation (30–40 W m⁻², S_{irrad} 0.05 m²) was quite similar.
- The lower the initial concentration of the contaminants in SE, the higher their indirect photolysis. Lower concentration also favoured the removal of pollutants and SE mineralization by CF1/Radiation (photocatalytic oxidation).
- CF1/O₃/Radiation system (photocatalytic ozonation) was the most efficient. Neither synergism nor antagonism between O₃/Radiation and CF1/Radiation systems was observed.
- In SE, the activity of the supported photocatalyst was much higher than that of P25.
- Supported catalysts showed good stability after three consecutive CF1/O₃/Radiation runs.

CRedit authorship contribution statement

Conceptualization: FJB, EMR, EMC, MF; Methodology: EMR, FJB; Validation: MF, EMR; Formal analysis: MF, EMR; Investigation: MF, EMR, EMC; Resources: FJB, EMR; Writing – original draft: EMR; Writing – review & editing: MF, EMR, EMC, FJB; Visualization: MF, EMR; Supervision: EMR; Project administration: FJB; Funding acquisition: FJB.

Declaration of Competing Interest

The authors declare that they have no known competing financial interests or personal relationships that could have appeared to influence the work reported in this paper.

Acknowledgements

The authors thank Agencia Estatal de Investigación of Spain co-financed by the European Funds for Regional Development (FEDER, EU) (project CTQ2015/64944R) and Agencia Estatal de Investigación of Spain (project PID2019-104429RB-I00/AEI/10.13039/501100011033) for the economic support. Manuel Alfredo Figueredo Fernández is grateful to Ministerio de Economía y Competitividad of Spain for his predoctoral grant (Resolution 28/03/2017, BOE no. 217, of 08/09/2016, reference number BES-2016-078456).

Appendix A. Supporting information

Supplementary data associated with this article can be found in the online version at [doi:10.1016/j.jece.2022.107371](https://doi.org/10.1016/j.jece.2022.107371).

References

- [1] S. Malato, P. Fernández-Ibáñez, M.I. Maldonado, J. Blanco, W. Gernjak, Decontamination and disinfection of water by solar photocatalysis: recent overview and trends, *Catal. Today* 147 (2009) 1–59, <https://doi.org/10.1016/j.cattod.2009.06.018>.
- [2] A.L. Linsebigler, A.L. Linsebigler, J.T. Yates Jr., G. Lu, G. Lu, J.T. Yates, Photocatalysis on TiO₂ surfaces: principles, mechanisms, and selected results, *Chem. Rev.* 95 (1995) 735–758, <https://doi.org/10.1021/cr00035a013>.
- [3] D. Kanakaraju, B.D. Glass, M. Oelgemöller, Advanced oxidation process-mediated removal of pharmaceuticals from water: a review, *J. Environ. Manag.* 219 (2018) 189–207, <https://doi.org/10.1016/j.jenvman.2018.04.103>.
- [4] M. Mehrjoui, S. Müller, D. Möller, A review on photocatalytic ozonation used for the treatment of water and wastewater, *Chem. Eng. J.* 263 (2015) 209–219, <https://doi.org/10.1016/j.cej.2014.10.112>.
- [5] A. Suligoj, M. Kete, U. Černigoj, F. Fresno, U. Lavrenčić Stangar, Synergism in TiO₂ photocatalytic ozonation for the removal of dichloroacetic acid and thiacloprid, *Environ. Res.* 197 (2021), 110982, <https://doi.org/10.1016/j.envres.2021.110982>.
- [6] E.M. Rodríguez, G. Fernández, P.M. Alvarez, F.J. Beltrán, TiO₂ and Fe (III) photocatalytic ozonation processes of a mixture of emergent contaminants of water, *Water Res.* 46 (2012) 152–166, <https://doi.org/10.1016/j.watres.2011.10.038>.
- [7] M. Fathinia, A. Khataee, Photocatalytic ozonation of phenazopyridine using TiO₂ nanoparticles coated on ceramic plates: mechanistic studies, degradation intermediates and ecotoxicological assessments, *Appl. Catal. A Gen.* 491 (2015) 136–154, <https://doi.org/10.1016/j.apcata.2014.10.049>.
- [8] M. Figueredo, E.M. Rodríguez, J. Rivas, F.J. Beltrán, Photocatalytic ozonation in water treatment: Is there really a synergy between systems? *Water Res.* 206 (2021) 1–13, <https://doi.org/10.1016/j.watres.2021.117727>.
- [9] E. Mena, A. Rey, F.J. Beltrán, TiO₂ photocatalytic oxidation of a mixture of emerging contaminants: a kinetic study independent of radiation absorption based on the direct-indirect model, *Chem. Eng. J.* 339 (2018) 369–380, <https://doi.org/10.1016/j.cej.2018.01.122>.
- [10] P. Wang, Aggregation of TiO₂ nanoparticles in aqueous media: effects of pH, ferric ion and humic acid, *Int. J. Environ. Sci. Nat. Resour.* 1 (2017) 157–162, <https://doi.org/10.19080/ijesnr.2017.01.555575>.
- [11] K. Doudrick, K.D. Hristovski, P.K. Westerhoff, Photocatalytic reduction of oxoanions, Patent US 9, 751, 785 B2, (2017).
- [12] P. Fernández-Ibáñez, J. Blanco, S. Malato, F.J. De Las Nieves, Application of the colloidal stability of TiO₂ particles for recovery and reuse in solar photocatalysis, *Water Res.* 37 (2003) 3180–3188, [https://doi.org/10.1016/S0043-1354\(03\)00157-X](https://doi.org/10.1016/S0043-1354(03)00157-X).
- [13] A.M. Chávez, D.H. Quiñones, A. Rey, F.J. Beltrán, P.M. Álvarez, Simulated solar photocatalytic ozonation of contaminants of emerging concern and effluent organic matter in secondary effluents by a reusable magnetic catalyst, *Chem. Eng. J.* 398 (2020), 125642, <https://doi.org/10.1016/j.cej.2020.125642>.
- [14] P. Singh, K. Sharma, V. Hasija, V. Sharma, S. Sharma, P. Raizada, M. Singh, A. K. Saini, A. Hosseini-Bandegharaei, V.K. Thakur, Systematic review on applicability of magnetic iron oxides-integrated photocatalysts for degradation of organic pollutants in water, *Mater. Today Chem.* 14 (2019), 100186, <https://doi.org/10.1016/j.mtchem.2019.08.005>.
- [15] B. Srikanth, R. Goutham, R. Badri Narayan, A. Ramprasad, K.P. Gopinath, A. R. Sankaranarayanan, Recent advancements in supporting materials for immobilised photocatalytic applications in waste water treatment, *J. Environ. Manag.* 200 (2017) 60–78, <https://doi.org/10.1016/j.jenvman.2017.05.063>.
- [16] L. Paredes, S. Murgolo, H. Dzinun, M.H. Dzarfan Othman, A.F. Ismail, M. Carballa, G. Mascolo, Application of immobilized TiO₂ on PVDF dual layer hollow fibre membrane to improve the photocatalytic removal of pharmaceuticals in different water matrices, *Appl. Catal. B Environ.* 240 (2019) 9–18, <https://doi.org/10.1016/j.apcatb.2018.08.067>.
- [17] A.Y. Shan, T.I.M. Ghazi, S.A. Rashid, Immobilisation of titanium dioxide onto supporting materials in heterogeneous photocatalysis: a review, *Appl. Catal. A Gen.* 389 (2010) 1–8, <https://doi.org/10.1016/j.apcata.2010.08.053>.
- [18] K. Tanaka, K. Abe, T. Hisanaga, Photocatalytic water treatment on immobilized TiO₂ combined with ozonation, *J. Photochem. Photobiol. A Chem.* 101 (1996) 85–87, [https://doi.org/10.1016/S1010-6030\(96\)04393-6](https://doi.org/10.1016/S1010-6030(96)04393-6).
- [19] M. Vargová, G. Plesch, U.F. Vogt, M. Zahoran, M. Gorbár, K. Jeseník, TiO₂ thick films supported on reticulated macroporous Al₂O₃ foams and their photoactivity in phenol mineralization, *Appl. Surf. Sci.* 257 (2011) 4678–4684, <https://doi.org/10.1016/j.apsusc.2010.12.121>.
- [20] M. Jiménez, M. Ignacio Maldonado, E.M. Rodríguez, A. Hernández-Ramírez, E. Saggiaro, I. Carra, J.A. Sánchez Pérez, Supported TiO₂ solar photocatalysis at semi-pilot scale: degradation of pesticides found in citrus processing industry wastewater, reactivity and influence of photogenerated species, *J. Chem. Technol. Biotechnol.* 90 (2015) 149–157, <https://doi.org/10.1002/jctb.4299>.
- [21] E.M. Rodríguez, A. Rey, E. Mena, F.J. Beltrán, Application of solar photocatalytic ozonation in water treatment using supported TiO₂, *Appl. Catal. B Environ.* 254 (2019) 237–245, <https://doi.org/10.1016/j.apcatb.2019.04.095>.
- [22] E. Lee, C.M. Glover, F.L. Rosario-Ortiz, Photochemical formation of hydroxyl radical from effluent organic matter: role of composition, *Environ. Sci. Technol.* 47 (2013) 12073–12080, <https://doi.org/10.1021/es402491t>.
- [23] S. Mostafa, F.L. Rosario-Ortiz, Singlet oxygen formation from wastewater organic matter, *Environ. Sci. Technol.* 47 (2013) 8179–8186, <https://doi.org/10.1021/es401814s>.

- [24] H. Zhou, S. Yan, L. Lian, W. Song, Triplet-state photochemistry of dissolved organic matter: triplet-state energy distribution and surface electric charge conditions, *Environ. Sci. Technol.* 53 (2019) 2482–2490, <https://doi.org/10.1021/acs.est.8b06574>.
- [25] D. Zhang, S. Yan, W. Song, Photochemically induced formation of reactive oxygen species (ROS) from effluent organic matter, *Environ. Sci. Technol.* 48 (2014) 12645–12653, <https://doi.org/10.1021/es5028663>.
- [26] H. Zhou, L. Lian, S. Yan, W. Song, Insights into the photo-induced formation of reactive intermediates from effluent organic matter: the role of chemical constituents, *Water Res.* 112 (2017) 120–128, <https://doi.org/10.1016/j.watres.2017.01.048>.
- [27] J. Mack, J.R. Bolton, Photochemistry of nitrite and nitrate in aqueous solution: a review, *J. Photochem. Photobiol. A Chem.* 128 (1999) 1–13, [https://doi.org/10.1016/S1010-6030\(99\)00155-0](https://doi.org/10.1016/S1010-6030(99)00155-0).
- [28] H. Strehlow, I. Wagner, Flash photolysis in aqueous nitrite solutions, *Z. Fur Phys. Chem.* 132 (1982) 151–160, <https://doi.org/10.1524/zpch.1982.132.2.151>.
- [29] J.J. Jankowski, D.J. Kieber, K. Mopper, Nitrate and nitrite ultraviolet actinometers, *Photochem. Photobiol.* 70 (1999) 319–328, <https://doi.org/10.1111/j.1751-1097.1999.tb08143.x>.
- [30] R. Andreozzi, V. Caprio, R. Marotta, D. Vogna, Paracetamol oxidation from aqueous solutions by means of ozonation and H₂O₂/UV system, *Water Res.* 37 (2003) 993–1004, [https://doi.org/10.1016/S0043-1354\(02\)00460-8](https://doi.org/10.1016/S0043-1354(02)00460-8).
- [31] S. Mandal, Reaction rate constants of hydroxyl radicals with micropollutants and their significance in advanced oxidation processes, *J. Adv. Oxid. Technol.* 21 (2018), <https://doi.org/10.26802/jaots.2017.0075>.
- [32] M. Bourgin, E. Borowska, J. Helbing, J. Hollender, H.-P. Kaiser, C. Kienle, C. S. McArdell, E. Simon, U. von Gunten, Effect of operational and water quality parameters on conventional ozonation and the advanced oxidation process O₃/H₂O₂: kinetics of micropollutant abatement, transformation product and bromate formation in a surface water, *Water Res.* 122 (2017) 234–245, <https://doi.org/10.1016/j.watres.2017.05.018>.
- [33] B.A. Wols, C.H.M. Hofman-Caris, Review of photochemical reaction constants of organic micropollutants required for UV advanced oxidation processes in water, *Water Res.* 46 (2012) 2815–2827, <https://doi.org/10.1016/j.watres.2012.03.036>.
- [34] R. Broséus, S. Vincent, K. Aboufadel, A. Daneshvar, S. Sauvé, B. Barbeau, M. Prévost, M. Prévost, Ozone oxidation of pharmaceuticals, endocrine disruptors and pesticides during drinking water treatment, *Water Res.* 43 (2009) 4707–4717, <https://doi.org/10.1016/j.watres.2009.07.031>.
- [35] M.M. Huber, S. Canonica, G.Y. Park, U. von Gunten, Oxidation of pharmaceuticals during ozonation and advanced oxidation processes, *Environ. Sci. Technol.* 37 (2003) 1016–1024, <https://doi.org/10.1021/es025896h>.
- [36] F.J. Real, J.L. Acero, F.J. Benitez, G. Roldán, L.C. Fernández, Oxidation of hydrochlorothiazide by UV radiation, hydroxyl radicals and ozone: kinetics and elimination from water systems, *Chem. Eng. J.* 160 (2010) 72–78, <https://doi.org/10.1016/j.cej.2010.03.009>.
- [37] F.J. Benitez, J.L. Acero, F.J. Real, G. Roldán, Ozonation of pharmaceutical compounds: rate constants and elimination in various water matrices, *Chemosphere* 77 (2009) 53–59, <https://doi.org/10.1016/j.chemosphere.2009.05.035>.
- [38] F.J. Rivas, J. Sagasti, A. Encinas, O. Gimeno, Contaminants abatement by ozone in secondary effluents. Evaluation of second-order rate constants, *J. Chem. Technol. Biotechnol.* 86 (2011) 1058–1066, <https://doi.org/10.1002/jctb.2609>.
- [39] M.C. Dodd, M.O. Buffle, U. von Gunten, Oxidation of antibacterial molecules by aqueous ozone: moiety-specific reaction kinetics and application to ozone-based wastewater treatment, *Environ. Sci. Technol.* 40 (2006) 1969–1977, <https://doi.org/10.1021/es051369x>.
- [40] R. Rosal, A. Rodríguez, J.A. Perdígón-Melón, A. Petre, E. García-Calvo, M. J. Gómez, A. Agüera, A.R. Fernández-Alba, Occurrence of emerging pollutants in urban wastewater and their removal through biological treatment followed by ozonation, *Water Res.* 44 (2010) 578–588, <https://doi.org/10.1016/j.watres.2009.07.004>.
- [41] J. Hoigné, H. Bader, W.R. Haag, J. Staehelin, Rate constants of reactions of ozone with organic and inorganic compounds in water-III. Inorganic compounds and radicals, *Water Res.* 19 (1985) 993–1004, [https://doi.org/10.1016/0043-1354\(85\)90368-9](https://doi.org/10.1016/0043-1354(85)90368-9).
- [42] M.A. Figueredo, E.M. Rodríguez, M. Checa, F.J. Beltran, Ozone-based advanced oxidation processes for primidone removal in water using simulated solar radiation and TiO₂ or WO₃ as photocatalyst, *Molecules* 24 (2019) 1728, <https://doi.org/10.3390/molecules24091728>.
- [43] J. Krýsa, G. Waldner, H. Měšťánková, J. Jirkovský, G. Grabner, Photocatalytic degradation of model organic pollutants on an immobilized particulate TiO₂ layer. Roles of adsorption processes and mechanistic complexity, *Appl. Catal. B Environ.* 64 (2006) 290–301, <https://doi.org/10.1016/j.apcatb.2005.11.007>.
- [44] J.T. Schneider, D.S. Firak, R.R. Ribeiro, P. Peralta-Zamora, Use of scavenger agents in heterogeneous photocatalysis: truths, half-truths, and misinterpretations, *Phys. Chem. Chem. Phys.* 22 (2020) 15723–15733, <https://doi.org/10.1039/d0cp02411b>.
- [45] I. Ivanova, C.B. Mendive, D. Bahnemann, The role of nanoparticulate agglomerates in TiO₂ photocatalysis: degradation of oxalic acid, *J. Nanopart. Res.* 18 (2016) 1–13, <https://doi.org/10.1007/s11051-016-3495-x>.
- [46] M. Kovacic, D. Juretic Perisic, M. Biosic, H. Kusic, S. Babic, A. Loncaric Bozic, UV photolysis of diclofenac in water: kinetics, degradation pathway and environmental aspects, *Environ. Sci. Pollut. Res.* 23 (2016) 14908–14917, <https://doi.org/10.1007/s11356-016-6580-x>.
- [47] G. Leo, C. Hi-Shi, D. Johnson, Light degradation of ketorolac tromethamine, *Int. J. Pharm.* 41 (1988) 105–113, [https://doi.org/10.1016/0378-5173\(88\)90142-1](https://doi.org/10.1016/0378-5173(88)90142-1).
- [48] R. Gurke, M. Röbler, C. Marx, S. Diamond, S. Schubert, R. Oertel, J. Fauler, Occurrence and removal of frequently prescribed pharmaceuticals and corresponding metabolites in wastewater of a sewage treatment plant, *Sci. Total Environ.* 532 (2015) 762–770, <https://doi.org/10.1016/j.scitotenv.2015.06.067>.
- [49] S. Dey, F. Bano, A. Malik, Pharmaceuticals and Personal Care Product (PPCP) Contamination-a Global Discharge Inventory, Elsevier Inc., 2019, <https://doi.org/10.1016/B978-0-12-816189-0.00001-9>.
- [50] I. Muñoz, M.J. Gómez-Ramos, A. Agüera, A.R. Fernández-Alba, J.F. García-Reyes, A. Molina-Díaz, Chemical evaluation of contaminants in wastewater effluents and the environmental risk of reusing effluents in agriculture, *TrAC Trends Anal. Chem.* 28 (2009) 676–694, <https://doi.org/10.1016/j.trac.2009.03.007>.